Exploration of Ti_3C_2Tz@Nickel Oxide Composite as a Supercapacitor Material

Beke Michael Abraham, Nelson Ebitei Sintei, Neminebor John, Tamadu Jasper Obi, Yabefa Akpodoitei Jeremiah
Email: beke.michael@gmail.com
DOI: 10.56201/ijccp.vol.11.no3.2025.pg54.62

Abstract
The burgeoning demand for efficient and high-performance energy storage devices has propelled research into novel materials capable of enhancing energy and power density. MXenes are a class of two-dimensional transition metal carbides/nitrides that have garnered significant attention in energy storage fabrication due to their excellent electrical conductivity, large surface area, and tunable surface chemistry. However, their tendency to restack limits their full potential. Nickel oxide (NiO), a transition metal oxide, offers high theoretical capacitance, it is in abundance, and it is also environmentally friendly, but it suffers from low electrical conductivity and poor cycling stability. This study presents the fabrication and application of MXene-nickel oxide (Ti3C2Tz -NiO) composites for enhanced supercapacitors. The synergistic combination of MXenes and NiO leverage on the superior electrical transport properties and mechanical strength of Ti3C2Tz to overcome the conductivity limitations of NiO, while the pseudocapacitive nature of NiO contributes to high energy density. The results shows that the composite exhibited a very high specific capacitance of 1050 F/g and an energy density of 81Wh/kg, which implies large energy storage capability. It also has a very low internal resistance of 0.4Ω, this means fast ion kinetics which is ideal for supercapacitors. It also demonstrated excellent electrochemical stability in a Galvanostatic charge-discharge measurement, it retained a capacitance of 97% after 3000 cycles. The results of the study reveal the exceptionally impressive potentials of the Mxene-NiO composite for supercapacitor applications

Keywords: *Mxene-Nickel Oxide, Batteries, Supercapacitor, Synergistic effect, Composite.*

1. Introduction

The pervasive reliance on fossil fuels and their detrimental environmental impact, coupled with an ever-increasing global energy consumption, underscore the urgent need for sustainable and efficient energy storage technologies. Supercapacitors and batteries are at the forefront of these advancements, offering solutions for a diverse range of applications, from portable electronics and electric vehicles to grid-scale energy storage systems[1–3]. While significant progress has been made in improving the performance of these devices, the demand for higher energy density, power density, and longer cycle life continues to drive research into novel materials and composite architectures[4–6].

Two-dimensional (2D) material has emerged as promising candidates for energy storage due to their unique structural and electronic properties. Among these, MXenes, a relatively new family of 2D transition metal carbides, nitrides, and carbonitrides, have attracted considerable interest since their discovery in 2011[7–9]. Synthesized by selectively etching the "A" group element from the MAX phases, MXenes possess intriguing attributes such as high electrical conductivity, large specific surface area, tunable surface terminations (e.g., -O, -OH, -F), and

excellent mechanical flexibility[10–13]. These characteristics make them highly suitable for electrochemical energy storage applications, facilitating rapid ion transport and electron transfer[14,15]. However, a significant challenge associated with pristine MXenes is their inherent tendency to restack due into van der Waals forces, which can reduce their accessible surface area and hinder ion diffusion, thereby limiting their full electrochemical performance[10,16–18]. To overcome these limitations and enhance their electrochemical properties, the integration of MXenes with other active materials has proven to be an effective strategy. Nickel oxide (NiO) is a widely investigated transition metal oxide for energy storage due to its high theoretical specific capacitance (2510 F g^{-1}), cost-effectiveness, abundance, and environmental benignity[19]. NiO exhibits pseudocapacitive behaviour originating from fast Faradaic redox reactions, contributing to high energy density[20,21]. Nevertheless, its practical application is often constrained by its low intrinsic electrical conductivity and poor cycling stability, which limit charge transfer kinetics and lead to capacity degradation over prolonged cycling [8].

The synergistic combination of MXenes and NiO presents a compelling approach to develop advanced composite materials for high-performance energy storage devices. By forming a hybrid structure, MXenes can provide an excellent conductive framework that will facilitate ion transport and mitigate the aggregation of NiO nanoparticles, while NiO contributes significant pseudocapacitance, thereby boosting the overall energy density[17,19,22]. In this study, we explore the fabrication of Ti_3C_2Tz@NiO composites and its application for high performance supercapacitor.

2. Materials and Methods

Materials

Ti_3AlC_2, NiO, HF, HCl, $Ni(NO_3)_2.6H_2O$, NH_4OH, Deionized water, LiF, NiO and C_2H_5OH.

2.1 Synthesis of Ti3C2Tz@NiO Composites

2.2 Preparation of Ti3C2Tz

The Ti_3C_2Tz is synthesized by selective etching of Ti_3AlC_2. An etching solution is first prepared to remove the Al from the Ti_3AlC_2 precursor. 1.0 g of LiF is dissolved in 9.0 ml of concentrated HCl and stirred for 30 minutes to complete the dissolution of the LiF. 1.0 g of Ti_3AlC_2 was added to the etching solution and allowed to react for 24 hours at room temperature. The Al is selectively removed from the precursor producing Ti_3C_2. The solution is then washed until a neutral pH is reached. The $Ti_3C_2T_z$ is filtered off and dried in an oven at 60ºC for 12 hours.

2.3 Preparation of NiO

4.0g of $Ni(NO_3)_2.6H_2O$ is dissolved in 100ml of deionized water, NH_4OH is added to the solution until a pH of 8 is reached. This result in the formation of $Ni(OH)_2$, which is transferred into a Teflon-lined autoclave and heated to 120ºC for 6 hours, allowing the $Ni(OH)_2$ to precipitate. It is then filtered off, washed with deionized water and ethanol and dried at 60ºC for 12 hours. The dried $Ni(OH)_2$ is then calcinated at 350ºC for 3 hours in a muffle furnace to obtain NiO.

2.4 Preparation of Ti3C2Tz/NiO Composites

A 1:1 ratio by weight of Ti3C2Tz and NiO are measured and transferred into a mortar and blended to for a uniform mix. A small amount of ethanol is added to the mixture to form a slurry and ultrasonicated for 30 minutes. This is then dried at 60ºC until a dry composite is obtained. Finally, to ensure a well-defined phase and improved structure, the composite is

calcinated at 400ºC for 2 hours. This enhances the interfacial contact and stability of the composite.

3 Characterization

3.1 FTIR

The FTIR spectrum of the composite displays MXene peaks at –OH (3400 cm^{-1}), -C-C-(1620 cm^{-1}), and –F (1100 cm^{-1})[23–25]. The peak at 550 cm^{-1} is associated with NiO[26,27]. The spectrum showed that all components are present in the composite, indicating a successful synthesis, it also suggests interaction between the MXene and NiO. Figure 1 is the FTIR spectrum of the composite.

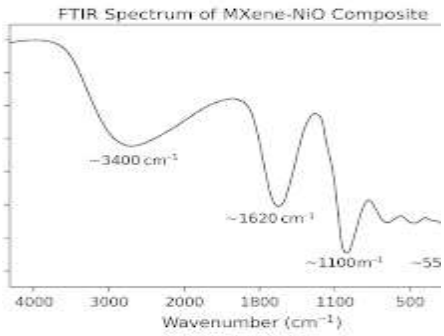


Figure 1, FTIR spectrum of the composite

3.2 X-ray Diffraction (XRD)

XRD was employed to determine the crystallinity and phase composition of the synthesized materials. The spectrum of the XRD of the composite has three distinctive peaks, the band at (00) peak at about 2Θ 16°, confirms the presence of MXene material[28,29]. The other peak (111) with reduced intensity at 2Θ 46°, is associated with NiO[20,22]. The XRD profile suggest a crystalline material. The XRD pattern of the composite is shown in Figure 2.

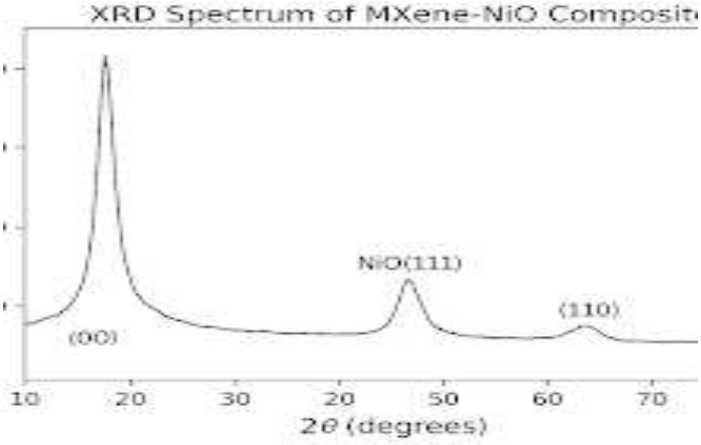


Figure 2, XRD spectrum of the composite

3.3 Scanning Electron Microscopy (SEM)

Sem was used to examine the surface morphology and particle size of the composite. The SEM images of the composite show a layer of flaky morphology for MXene, while that of the composite exhibited a coating of the NiO over the MXene layers. Figure 3 displays the SEM images of the composite.

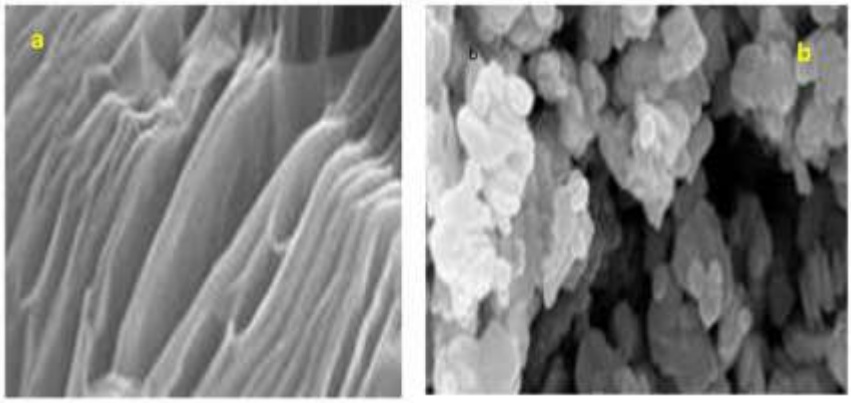


Figure 3, Sem images of (a) Mxene and (b) composite

3.4 Brunauer-Emmett-Teller (BET)

BET was employed to measure the surface area and porosity of the composite. The BET analysis results showed that the surface area of the composite is 222 m^2/g. This could be attributed to the intercalated morphology of the composite. The pore size distribution (BJH method) showed mesopores with an average pore size of 4.0 nm. The Isotherm of the composite is displayed in Figure 4.

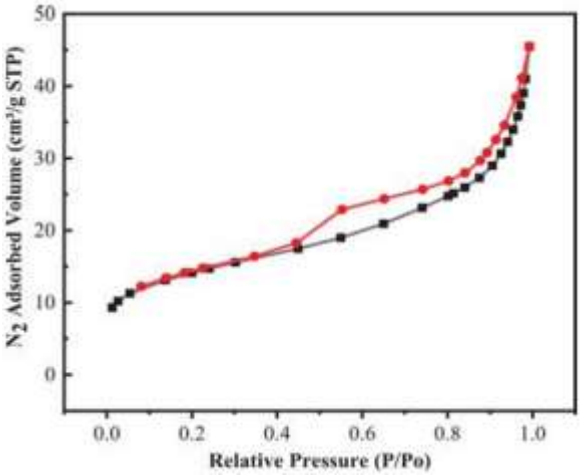


Figure 4, BET Isotherm of the composite material

4 Electrochemical Analysis

The electrochemical properties of the composite material were analysed by Cyclic Voltammetry (CV), Electrochemical Impedance Spectroscopy (EIS), and Galvanostatic charge discharge (GCD).

4.1 Cyclic Voltammetry (CV)

CV was employed to investigate the charge storage mechanism and specific capacitance of the composite material. A three electrode Galvanostatic workstation was used, the electrolyte was a 2.0M H_2SO_4 solution. The potential window was (-0.7 - +0.7) V. The CV curve of the composite is displayed in Figure 5. It shows that the composite undergoes REDOX reaction which is ideal for charge-discharge[30,31]. The shape of the curve also suggests the presence of Electric Double Layer capacitance (EDLC)[32] likely from the Mxene component, and

Pseudocapacitance from the Nickel Oxide[33,34]. The synergistic effect of combining a conductive MXene and a pseudocapacitive metal oxide enhanced the charge storage capacity of the composite. A specific capacitance of 1050 F/g at a scan rate of 5 mV/s was achieved. This demonstrates the great potential of the composite as an effective material for energy storage device.

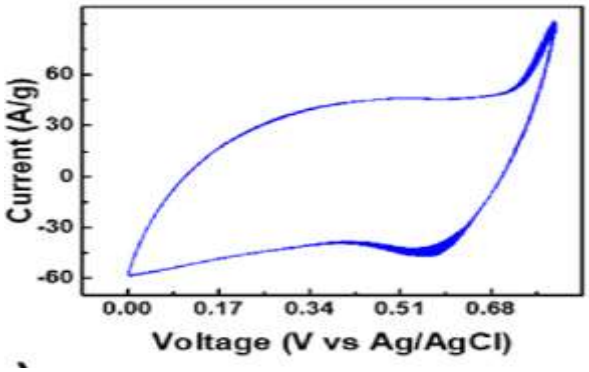


Figure 5, CV curve of the composite

4.2 Galvanostatic Charge Discharge (GCD)

GCD was used to evaluate the energy and power densities as well as electrochemical stability of the composite. The GCD curves of the composite material at different potential is displayed in Figure 6. The energy density of the composite is 81 Wh/kg, and after 3000 cycles of charge-discharge it retained 97% capacitance. The impressive current density and electrochemical stability exhibited by the composite implies it is a suitable material for energy storage.

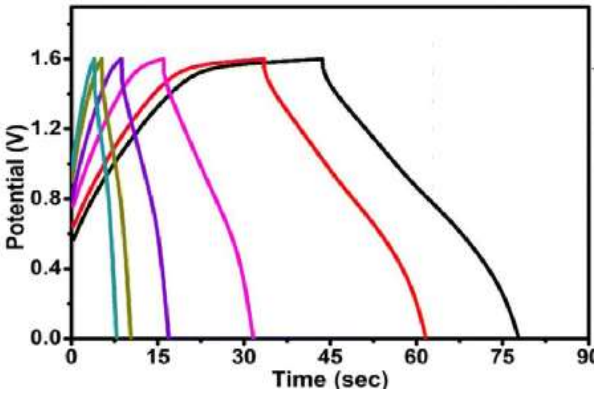


Figure 7, GCD curves of the composite at different potentials

4.3 Electrochemical Impedance Spectroscopy (EIS)

EIS was employed to investigate the internal resistance and charge transfer dynamics within the composite material. The result shows that the composite exhibited a very low internal resistance of 0.4Ω, and the dimension of the semi-circle in the Nyquist plot shows it has a fast ion kinetics. All three electrochemical analysis shows that the composite is an excellent material for energy storage application. Figure 8 shows the Nyquist plot of the composite material,

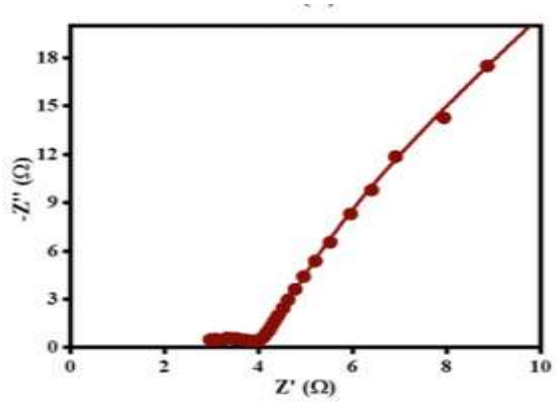


Figure 8, Nyquist plot of the composite material

5 Conclusion

This study unveils the novel Ti_3C_2Tz@NiO composite as a high-performing material for supercapacitor applications. The synergistic interactions between the MXene and nickel oxide were explored in energy storage technology. The Ti_3C_2Tz/@NiO was successfully fabricated and investigated for use as a supercapacitor. The result was very impressive, the specific capacitance of the composite at a scan rate of 5 mV/s is 1050 F/g, with an energy density of 81 Wh/kg and an internal resistance is 0.4Ω. The results shows that the composite will perform exceptionally as a supercapacitor, with a very large energy storage capability and fast ion kinetics which are ideal properties for energy storage devices. It also exhibited excellent electrochemical stability, the Galvanostatic charge-discharge test shows a capacitance retention of 97% after 3000 cycles. These results showcase Ti_3C_2Tz@NiO as a very strong material for high performance supercapacitor application.

Conflict of Interest: The authors declare that there is no conflict of interest.
Funding: The research is funded by the authors.

5. References

[1] D. Aradilla ∗, S. Sadki, G. Bidan, Beyond conventional supercapacitors: Hierarchically conducting polymer-coated 3D nanostructures for integrated on-chip micro-supercapacitors employing ionic liquid electrolytes, (2018). https://doi.org/10.1016/j.synthmet.2018.11.022.

[2] T.C. Girija, M. V Sangaranarayanan, Polyaniline-based nickel electrodes for electrochemical supercapacitors—Influence of Triton X-100, J Power Sources 159 (2006) 1519–1526. https://doi.org/https://doi.org/10.1016/j.jpowsour.2005.11.078.

[3] N. Kumar, S. Bin Kim, S.Y. Lee, S.J. Park, Recent Advanced Supercapacitor: A Review of Storage Mechanisms, Electrode Materials, Modification, and Perspectives, Nanomaterials 12 (2022). https://doi.org/10.3390/nano12203708.

[4] H. Zhang, J. Wang, Q. Shan, Z. Wang, S. Wang, Tunable electrode morphology used for high performance supercapacitor: Polypyrrole nanomaterials as model materials, Electrochim Acta 90 (2013) 535–541. https://doi.org/10.1016/J.ELECTACTA.2012.12.045.

[5] S. He, W. Chen, 3D graphene nanomaterials for binder-free supercapacitors: scientific design for enhanced performance, Nanoscale 7 (2015) 6957–6990. https://doi.org/10.1039/C4NR05895J.

[6] M. Almusawi, A. Shukla, S. Hemalatha, P. Kavitha, G.M. Gambhire, P.R. Pardeshi, B. Pragathi, Comparative Analysis of Supercapacitors vs. Batteries, in: E3S Web of Conferences, EDP Sciences, 2024. https://doi.org/10.1051/e3sconf/202459101010.

[7] G. Wang, L. Zhang, J. Zhang, A review of electrode materials for electrochemical supercapacitors, Chem Soc Rev 41 (2012) 797–828. https://doi.org/10.1039/C1CS15060J.

[8] L. Sun, Y. Dong, H. Li, H. Meng, J. Liu, Q. Cao, C. Pan, Research Progress and Challenges of Carbon/MXene Composites for Supercapacitors, Batteries 10 (2024). https://doi.org/10.3390/batteries10110395.

[9] K. Li, X. Wang, X. Wang, M. Liang, V. Nicolosi, Y. Xu, Y. Gogotsi, All-pseudocapacitive asymmetric MXene-carbon-conducting polymer supercapacitors, Nano Energy 75 (2020) 104971. https://doi.org/10.1016/J.NANOEN.2020.104971.

[10] R. Garg, A. Agarwal, M. Agarwal, Synthesis and optimisation of MXene for supercapacitor application, Journal of Materials Science: Materials in Electronics 31 (2020) 18614–18626. https://doi.org/10.1007/s10854-020-04404-5.

[11] W. Wei, X. Cui, W. Chen, D.G. Ivey, Manganese oxide-based materials as electrochemical supercapacitor electrodes, Chem Soc Rev 40 (2011) 1697–1721. https://doi.org/10.1039/C0CS00127A.

[12] S. Sun, L. Guo, X. Chang, Y. Yu, X. Zhai, MnO2/g-C3N4@PPy nanocomposite for high-performance supercapacitor, Mater Lett 236 (2019) 558–561. https://doi.org/10.1016/j.matlet.2018.11.001.

[13] N.K. Pavithra Siddu, S.M. Jeong, C.S. Rout, MXene-carbon based hybrid materials for supercapacitor applications, Energy Advances 3 (2024) 341–365. https://doi.org/10.1039/d3ya00502j.

[14] X. Chen, X. Wang, F. Liu, X. Song, H. Cui, Fabrication of NiO–ZnO-modified g-C3N4 hierarchical composites for high-performance supercapacitors, Vacuum 178 (2020). https://doi.org/10.1016/j.vacuum.2020.109453.

[15] P.M. Shafi, R. Dhanabal, A. Chithambararaj, S. Velmathi, A.C. Bose, α-MnO2/h-MoO3 Hybrid Material for High Performance Supercapacitor Electrode and Photocatalyst, ACS Sustain Chem Eng 5 (2017) 4757–4770. https://doi.org/10.1021/acssuschemeng.7b00143.

[16] Y. Li, C. Pan, P. Kamdem, X.-J. Jin, Binder-Free Two-Dimensional MXene/Acid Activated Carbon for High-Performance Supercapacitors and Methylene Blue Adsorption, Energy & Fuels 34 (2020) 10120–10130. https://doi.org/10.1021/acs.energyfuels.0c01352.

[17] I. Hussain, A. Hanan, F. Bibi, O.J. Kewate, M.S. Javed, K. Zhang, Non-Ti (M2X and M3X2) MXenes for Energy Storage/Conversion, Adv Energy Mater (2024). https://doi.org/10.1002/aenm.202401650.

[18] X. Li, F. Ran, F. Yang, J. Long, · Lu Shao, Advances in MXene Films: Synthesis, Assembly, and Applications, Transactions of Tianjin University 27 (2021) 217–247. https://doi.org/10.1007/s12209-021-00282-y.

[19] M. Van Tran, A.T. Ha, P.M.L. Le, Nanoflake manganese oxide and nickel-manganese oxide synthesized by electrodeposition for electrochemical capacitor, J Nanomater 2015 (2015). https://doi.org/10.1155/2015/609273.

[20] J.K. Kim, PEG-assisted sol-gel synthesis of compact nickel oxide hole-selective layer with modified interfacial properties for organic solar cells, Polymers (Basel) 11 (2019). https://doi.org/10.3390/polym11010120.

[21] K.A. Gandionco, J.W. Kim, J.D. Ocon, J. Lee, Activated carbon-nickel (II) oxide electrodes for capacitive deionization process, Applied Chemistry for Engineering 31 (2020) 552–559. https://doi.org/10.14478/ace.2020.1064.

[22] S. Pilban Jahromi, N.M. Huang, A. Kamalianfar, H.N. Lim, M.R. Muhamad, R. Yousefi, Facile synthesis of porous-structured nickel oxide thin film by pulsed laser deposition, J Nanomater 2012 (2012). https://doi.org/10.1155/2012/173825.

[23] Z. Chen, X. Xu, Z. Ding, K. Wang, X. Sun, T. Lu, M. Konarova, M. Eguchi, J.G. Shapter, L. Pan, Y. Yamauchi, Ti 3 C 2 MXenes-derived NaTi 2 (PO 4) 3 / MXene nanohybrid for fast and efficient hybrid capacitive deionization performance, 407 (2021).

[24] M. Naguib, V.N. Mochalin, M.W. Barsoum, Y. Gogotsi, 25th anniversary article: MXenes: A new family of two-dimensional materials, Advanced Materials 26 (2014) 992–1005. https://doi.org/10.1002/ADMA.201304138.

[25] A. Molaei Aghdam, N. Mikaeili Chahartagh, E. Delfani, High-Efficient Capacitive Deionization Using Amine-Functionalized ZIF-67@ 2D MXene: Toward Ultrahigh Desalination Performance, Adv Mater Technol 8 (2023). https://doi.org/10.1002/ADMT.202300628.

[26] A.M. Mahmoud, F.A. Ibrahim, S.A. Shaban, N.A. Youssef, Adsorption of heavy metal ion from aqueous solution by nickel oxide nano catalyst prepared by different methods, Egyptian Journal of Petroleum 24 (2015) 27–35. https://doi.org/10.1016/j.ejpe.2015.02.003.

[27] R.A. Raj, M.S. AlSalhi, S. Devanesan, Microwave-assisted synthesis of nickel oxide nanoparticles using Coriandrum sativum leaf extract and their structural-magnetic catalytic properties, Materials 10 (2017). https://doi.org/10.3390/ma10050460.

[28] Z. Chen, X. Xu, Z. Ding, K. Wang, X. Sun, T. Lu, M. Konarova, M. Eguchi, J.G. Shapter, L. Pan, Y. Yamauchi, Ti3C2 MXenes-derived NaTi2(PO4)3/MXene nanohybrid for fast and efficient hybrid capacitive deionization performance, Chemical Engineering Journal 407 (2021) 127148. https://doi.org/10.1016/J.CEJ.2020.127148.

[29] H. Xue, X. Gao, M.K. Seliem, M. Mobarak, R. Dong, X. Wang, K. Fu, Q. Li, Z. Li, Efficient adsorption of anionic azo dyes on porous heterostructured MXene/biomass activated carbon composites: Experiments, characterization, and theoretical analysis via advanced statistical physics models, Chemical Engineering Journal 451 (2023) 138735. https://doi.org/10.1016/J.CEJ.2022.138735.

[30] X. Su, T.A. Hatton, Redox-electrodes for selective electrochemical separations, Adv Colloid Interface Sci 244 (2017) 6–20. https://doi.org/10.1016/j.cis.2016.09.001.
[31] Y. Li, Z. Ding, J. Li, J. Li, T. Lu, L. Pan, Highly efficient and stable desalination via novel hybrid capacitive deionization with redox-active polyimide cathode, 469 (2019).
[32] B.-A. Mei, O. Munteshari, J. Lau, B. Dunn, L. Pilon, Physical Interpretations of Nyquist Plots for EDLC Electrodes and Devices, The Journal of Physical Chemistry C 122 (2017). https://doi.org/10.1021/acs.jpcc.7b10582.
[33] B.E. Conway, V. Birss, J. Wojtowicz, The role and utilization of pseudocapacitance for energy storage by supercapacitors, 66 (1997) 1–14.
[34] M. Gao, Z. Yang, W. Liang, T. Ao, W. Chen, Recent advanced freestanding pseudocapacitive electrodes for efficient capacitive deionization, Sep Purif Technol 324 (2023). https://doi.org/10.1016/J.SEPPUR.2023.124577.